Available online at www.sciencedirect.com
SCIENCE DIRECT
Polymer 46 (2005) 8624–8633
polymer
www.elsevier.com/locate/polymer

Synthesis and properties of liquid crystalline polymers with low T_m and broad mesophase temperature ranges

Bor-Kuan Chen[a,*], Sun-Yuan Tsay[a], Jun-Yuan Chen[b]

[a]*Department of Polymer Materials, Kun Shan University of Technology, Tainan 710, Taiwan, ROC*
[b]*Formosa Plastics Co. Ltd, Kaohsiung 814, Taiwan, ROC*

Received 12 May 2005; received in revised form 22 June 2005; accepted 22 June 2005
Available online 10 August 2005

Abstract

Novel thermotropic liquid crystalline polymers (TLCP) with improved processability and lower cost than Vectra® were synthesized by esterification and melt polycondensation. Aromatic compounds, 6-hydroxyl-2-naphthoic acid, 2,6-naphthlenedicarboxylic acid, 4-hydroxybenzoic acid or terephthalic acid, were used as polycyclic stiff rod-like mesogenic groups. Aliphatic diol, ethylene glycol or 1,4-butanediol was used as flexible spacers to form semi-flexible main chain TLCP. The LCP products were characterized by FT-IR and ^{1}H NMR to identify their chemical structures. The analytical results showed the polymers had inherent viscosities of 0.35–0.54 dL/g. The crank shaft structure of the naphthalene decreased the melting temperature (T_m) of LCP (181–272 °C) to facilitate extrusion or injection molding, and maintained relatively high heat deflection temperature for high performance engineering plastics applications. The 5% weight loss decomposition temperatures were above 400 °C. LCPs have good solvent resistance and low hygroscopicity. The SEM morphology showed strong orientation on the surface in the flow direction and many micro-fibers structure in a sectional drawing. The optical textures of polymers observed by POM revealed a strong birefringence in the melts and indicated that they form nematic mesophase. All polymers have broad mesophase temperature (ΔT_{meso}) ranges.

Keywords: Liquid crystalline polymer; Naphthalene; Melt polycondensation

1. Introduction

Liquid crystalline polymers (LCPs) with the qualities of high strength, stiffness and chemical resistance, good dimensional stability and low linear thermal expansion coefficient make them attractive high performance engineering materials [1,2]. LCPs consist of repeating mesogenic monomer units that are incorporated into the main-chain of a polymer backbone. The incorporation of a rigid structure of mesogenic units to the main-chain polymer gives rise to an increase in melting temperature, high modulus and high strength [3]. There are two major LCP types: One is lyotropic LCP, e.g. Kevlar based on poly(*p*-phenylene terephthalamide) [4], which forms liquid crystalline structure with a diluent (in solution); another is thermotropic LCP (TLCP), e.g. Vectra based on wholly aromatic polyester [5], which forms liquid crystalline structure upon heating. While the lyotropic LCP can be fabricated only in fibers or films, the thermotropic LCP can be made into a three-dimensional structure by conventional processing, such as injection molding. This makes TLCP a unique material for a wide range of applications [6]. However, LCPs with high melting temperature exhibit poor melt processability. Several researchers have devoted considerable efforts to modify the structure and properties of LC aromatic polyesters [7–9]. In order to reach more practical conditions for industrial processing, several approaches have been utilized to reduce the transition temperatures of LCPs. These include frustrated chain packing [10], flexible spacers [11], and nonlinear links [12]. The insertion of flexible segments or spacers to separate the mesogenic units along the polymer backbone is aimed to reduce the transition temperature and to preserve the chemical periodicity of the molecules of LCPs.

Vectra is a random copolyester of 4-hydroxybenzoic acid (HBA) and 6-hydroxy-2-naphthoic acid (HNA) with a

* Corresponding author. Tel.: +886 6 2051253; fax: +886 6 2756841.
E-mail address: chenbk@seed.net.tw (B.-K. Chen).

0032-3861/$ - see front matter © 2005 Elsevier Ltd. All rights reserved.
doi:10.1016/j.polymer.2005.06.084

faction of 73/27 (mol/mol), which gives rise to the nematic phase transition at melting temperature (T_m) of 285 °C from semi-crystalline phase [13]. We are developing novel TLCPs that have lower T_m, wider mesomorphoric temperature range, better processability and cost advantage than Vectra. These naphthalene containing TLCPs were synthesized by melt polymerization. 2,6-Naphthlenedicarboxylic acid (NDA) and terephthalic acid (TPA) were used to substitute the expensive HNA and HBA. Poly (methylene) flexible spacer was inserted to form a semi-flexible main chain. The crank shaft structure of the naphthalene in these LCPs decreased the melting point to facilitate extrusion or injection molding, while maintaining thermal stability. Our reaction scheme imitates the polyester process. In commercial process, polyester melt polymerized at temperature ~280 °C and it would not decompose until temperature higher than 350 °C. The LCP products were characterized by FT-IR and ^{1}H NMR to identify the chemical structures. TGA, DSC, and TMA were used to measure the thermal properties. X-ray diffractometer (XRD) and scanning electron microscopy (SEM) were utilized to study the morphology of the LCPs. The optical textures of polymers were investigated by POM. Their thermal behavior and liquid crystalline properties are presented and discussed.

2. Experimental

2.1. Materials

Chemicals of high purity were obtained from various commercial sources, which consisted of 6-hydroxy-2-naphthoic acid, 4-hydroxybenzoic acid (San Fu Chemical, Taiwan), acetic anhydride (Acros), ethylene glycol [EG], 1, 4-butanediol [BDO], terephthalic acid (Lancaster) and 2,6-naphthalene dicarboxylic acid [NDA] (Amoco). NDA was purified by dissolving in DMAc with activated carbon added, then filtered to remove the impurities. The needle crystalline NDA was obtained after cooling. HNA was further purified by dissolving in ethanol or 1,4-dioxane, and filtered to remove impurities. The purified HNA precipitated out by adding de-ionized water. Various catalysts and additives were used as received without any further purification, included sodium acetate, antimony(III)oxide (Acros), tetrabutyl orthotitanate (Fluka), triphenyl phosphite [TPP] (Lancaster) and Irganox 1010 (Ciba).

2.2. Monomer synthesis

The esterification was carried out in two stages. First, acetylation activated the acids; then the monomer was reacted with aliphatic diol to synthesize the ester.

2.2.1. Preparation of 4-acetoxybenzoic acid (ABA) and 6-acetoxy-2-naphthoic acid (ANA)

The monomers ABA and ANA were made by the acetylation of HBA and HNA separately, with acetic anhydride as solvent in the presence of a catalytic amount of sodium acetate [14]. The prepared monomer ABA was then purified by recrystallization. ANA was prepared in a similar procedure. The melting point of ABA was 193 °C and ANA was 240 °C (by DSC). ^{1}H NMR was used to confirm the success of the acetylation. The following absorptions correspond to different H in ABA molecule: Aromatic H: 7.3, 8.0 ppm; –CH_3: 2.3 ppm; –COOH: >10 ppm. And the absorptions for different H in ANA molecule were: Aromatic H: 7.4, 7.8, 8.0, 8.2, 8.7 ppm; –CH_3: 2.3 ppm; –COOH: >10 ppm.

2.2.2. Synthesis of esters with methylene spacer

ABA and ANA reacted with EG or BDO separately to form four monomers of LCP as shown in Scheme 1. ABA 90 g and EG 93 g (or BDO 68 g) in a molar ratio of 1:3 and

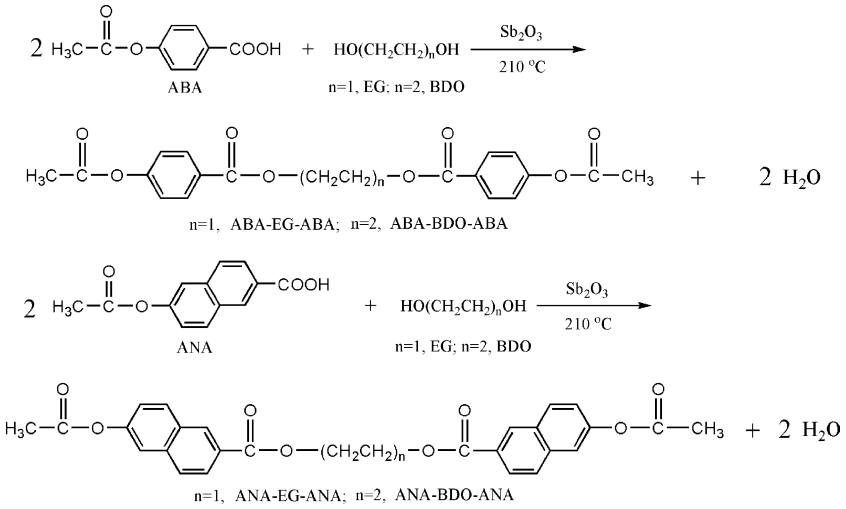

Scheme 1. Synthesis of esters with methylene spacers.

300 ppm of Sb_2O_3 catalyst were introduced into a four-neck glass flask, which was purged with nitrogen. The mixture was stirred at 200 rpm for 30 min, and was heated to 130 °C gradually. The mixture turned clear solution and then was continually heated to 210 °C. ABA and EG or BDO reacted to form ABA–EG–ABA or ABA–BDO–ABA. After stirred for 8–10 h under nitrogen, the reaction was completed upon the collection of ≧95% theoretical amount of water. The excess EG or BDO and water byproducts were withdrawn by aspirator. After the mixture was cooled to room temperature, the white product precipitated out. The product was washed with ice cold deionized water to remove the residual EG or BDO, then dried to give ABA–EG–ABA (86% yield) or ABA–BDO–ABA (71% yield). ANA–EG–ANA or ANA–BDO–ANA was synthesized by similar procedure.

2.3. Polymerization

A typical example of polymerization was executed as follows. A mixture of ABA–EG–ABA and NDA with a molar ratio of 1:1 and 250–300 ppm of Sb_2O_3 and $Ti(OBu)_4$ catalysts was placed in a flask equipped with a stainless steel stirrer and an inlet and an outlet for nitrogen. The nitrogen outlet was connected to a distillation column that led to a receiver with provision for applying vacuum. After the reaction flask was purged with nitrogen to remove all air, it was then heated to the melting point of the mixture (190–200 °C). To inhibit the decomposition of product in the later part of reaction, thermal stabilizer TPP and antioxidant Irganox 1010 were added. The flask was stirred at 200 rpm while the nitrogen flow was controlled to avoid the evaporation of reactants. After holding at 200 °C for 5 h, the content was heated gradually to 280 °C and acetic acid slowly distilled out. A vacuum was applied with an aspirator when no more distillate noticed. Until the pressure in the flask was reduced to 10 torr, an oil rotary vacuum pump was then employed to pull a vacuum below 2 torr while stirring continually for 4 h. The polymer obtained was ground and subjected to Soxhlet extraction for 16 h using acetone to remove monomers and oligomers, then dried under a vacuum.

Other polymers in this study (code is listed in Table 1) were prepared by similar procedures (Scheme 2). P1 and P2 use NDA as the diacid, while P3 and P4 use TPA as the diacid and substitute ABA with ANA.

2.4. Characterization

Fourier transfer infrared (FTIR) and ^1H NMR spectra were recorded on a Bio-rad FTS-40A and a Bruker 400 MHz spectrometer, respectively. Elemental analyses were carried out on a Heraus CHN rapid elemental analyzer. Thermo-gravimetric analysis (TGA) was performed with a Perkin–Elmer TGA-7 at a heating rate of 20 °C/min in N_2. Differential scanning calorimetry (DSC) data were obtained from a Perkin–Elmer DSC-7. Samples were scanned at a heating rate of 20 °C/min under N_2. Dynamic mechanical analysis (DMA) was performed on a Perkin–Elmer DMA-7 thermal analyzer. X-ray diffractograms were obtained on a Rigaku Flex D/Max IIIa instrument with Ni-filtered Cu K_α radiation. The inherent viscosities were measured using an Ubbelohde viscometer (Schott Gerate AVS310) at 30 °C. Qualitative solubility was determined by dissolving 0.5 g of polymer in 5 mL of solvent. For the measurement of hygroscopicity, specimens were exposed to boiling water for 8 h, and the weight difference was calculated after two more days in water at room temperature. Fibers were drawn as the polymer melted and were fractured cryogenically in liquid nitrogen. The morphologies of the fracture surfaces were observed with a Hitachi S-4100 SEM. Liquid crystalline textures were identified using a Nikon Labophot-Pol polarizing optical microscopy (POM) equipped with a Mettler FP84 heating stage and a Mettler FP80 control unit.

3. Results and discussion

3.1. Monomer syntheses via esterification

Most main-chain LCPs are polymerized through condensation (mostly transesterification) reactions. Before polymerization, monomers are usually acetylated to increase their reaction activities [15]. For the polycondensation of wholly aromatic polyesters, several effective catalysts are known to have the capabilities of accelerating the reaction, such as alkali metal acetate.

For the synthesis of ABA or ANA, HBA or HNA was reacted with acetic anhydride in the presence of sodium acetate catalyst. The formation of byproduct, acetic acid, will slow the reaction rate. To overcome it, excess amount of acetic anhydride was used as reactant as well as solvent.

Table 1
Code of liquid crystalline polymers and results of elemental analysis

Polymer code	Ester	Diacid	C (%)		H (%)	
			Calcd.	Found	Calcd.	Found
P1	ABA–EG–ABA	NDA	72.10	70.84	3.86	4.05
P2	ABA–BDO–ABA	NDA	72.87	70.43	4.45	4.32
P3	ANA–EG–ANA	TPA	74.42	72.54	3.88	4.06
P4	ANA–BDO–ANA	TPA	74.44	73.24	4.51	4.25

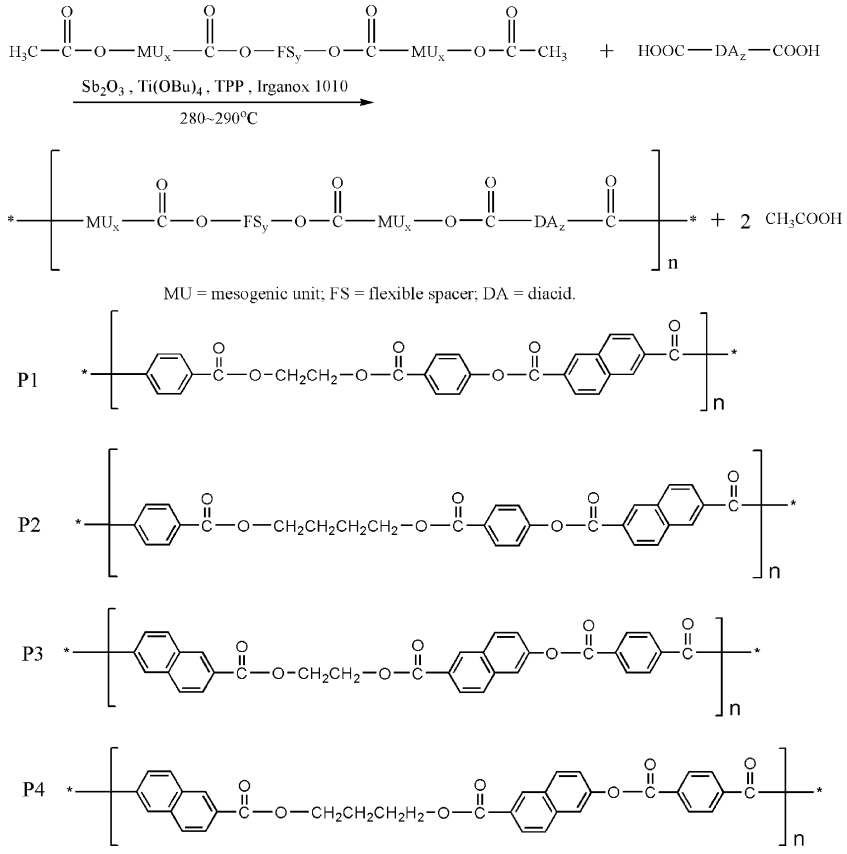

Scheme 2. Synthesis of polymers.

But, too much acetic anhydride was undesirable because of the cost and waste of raw material, and increased difficulty in product purification. The optimum molar ratio of HBA or HNA to acetic anhydride was found to be 1:2.5. For the esterification of ABA and ANA with EG or BDO diols, the reaction rate was slow; 300 ppm of Sb_2O_3 was found to be the optimum amount of catalyst [14,16]. Due to the low boiling point of diols and high reaction temperature

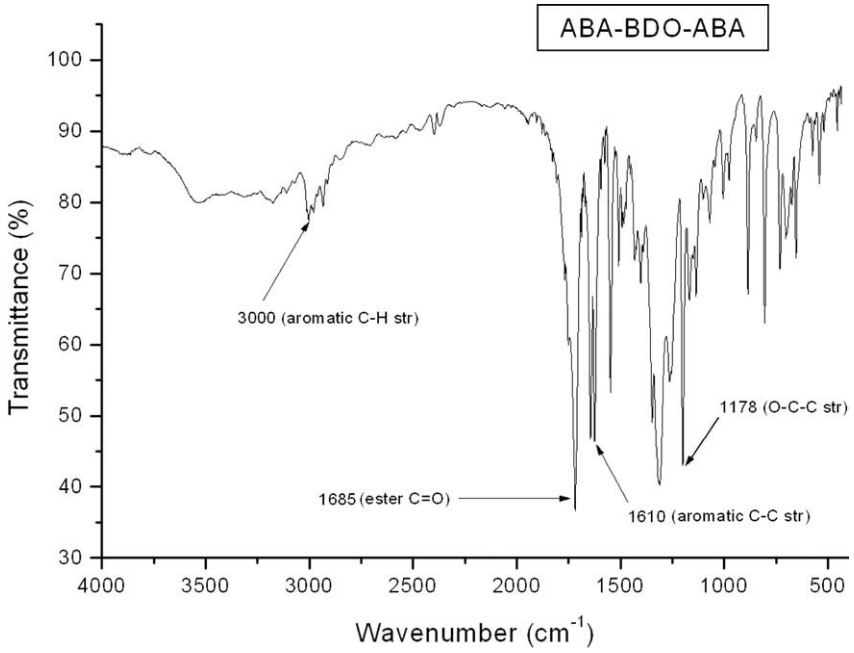

Fig. 1. IR spectrum of ABA–BDO–ABA.

(210 °C), the molar ratio of ABA or ANA to diols used was 1:3 to achieve a better reaction yield.

The structures of the esterification products were confirmed by IR and ^{1}H NMR. Fig. 1 shows the IR spectrum of ABA–BDO–ABA. IR (KBr) 3000 cm^{-1} (Ar C–H str), 1685 cm^{-1} (ester C=O), 1610 cm^{-1} (Ar C–C str), and 1178 cm^{-1} (O–C–C unsym str). For ^{1}H NMR (DMSO-d_6) of ANA–EG–ANA (as shown in Fig. 2), δ 7.1–8.5 (6H, naphthalenic), 2.0 (3H, –CH_3), 4.2–4.6 (4H, –CH_2), and 2.48 (solvent). All of the spectroscopic data obtained were in good agreement with the proposed structure.

3.2. Polymerization of LCPs

Since the melt polymerization of thermotropic LCP transitions from a homogenous phase to a heterogeneous system due to the separation of the liquid crystal (LC) phase from the isotropic melt, different LC textures associated with different defects can be observed [17]. The synthesis conditions can affect the LC texture and morphology, which determine the properties of final products. For the synthesis of P1 ~ P4 from ester monomers and diacids, NDA or TPA, the removal of acetic acid is one of the driving forces for polymer formation. The control of heating rate and nitrogen flow is also important to avoid the loss of reactants from evaporation. The vacuum applied in the polymerization can affect the degree of polymerization. A two-stage operation is essential. The vacuum should be maintained around 10 torr in the first stage during the prepolymerization, then reduced to 2 torr in the second stage and held for 4–5 h to form a high molecular weight LCP.

3.3. Characterization of LCPs

3.3.1. Elemental analyses

The results of the elemental analyses of all polymers synthesized are listed in Table 1. The values differ by 2–5% for the proposed structures. These differences can be accounted for by (1) loss of reactants, monomers or oligomers, from evaporation by the excess nitrogen flow or higher reaction temperature; (2) poor solubility of diacids and hence poor reactivity in the initial stage of polymerization; (3) difference in the reactivity of monomers during the polymerization, which lead to polymers with different compositions, the so called 'composition drift' [18].

3.3.2. NMR analyses

In general, the ^{1}H NMR spectra of the polymers are divided into two parts, with the first showing the aromatic (phenyl and naphthalenic) protons in the downfield region (6.8–8.7 ppm), and the second the methylene protons in the region of 4.3–4.7 ppm. A typical ^{1}H NMR ($CDCl_3$)

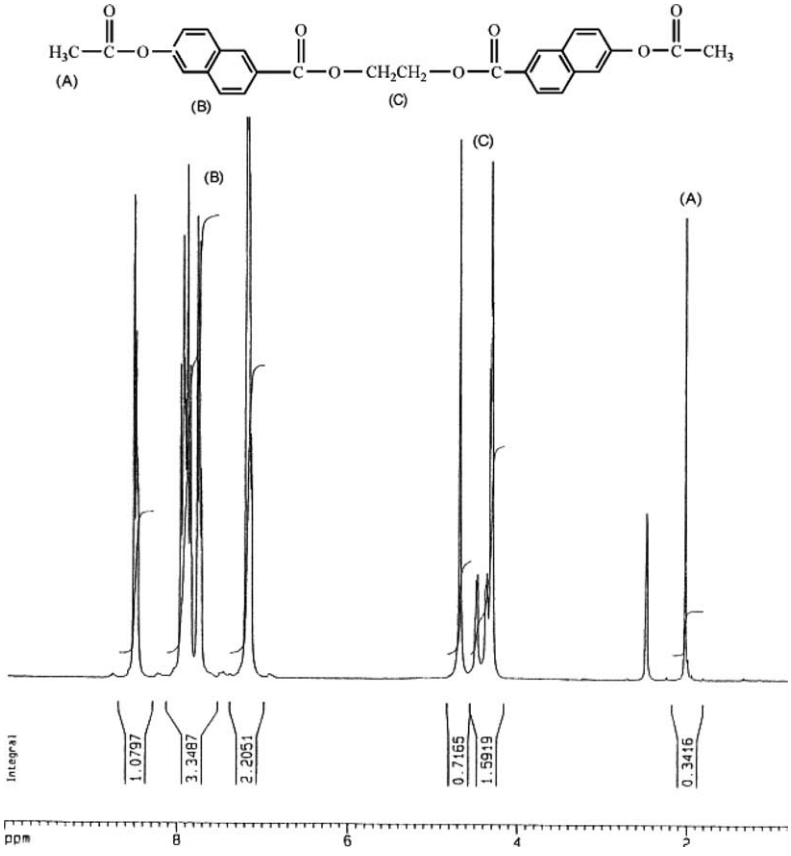

Fig. 2. ^{1}H NMR spectrum of ANA–EG–ANA.

spectrum, for polymer P3, is presented in Fig. 3. It elucidates the presence of the methylene groups in this polymer and the flexible spacers did not break during melt polycondensation with diacids. The analysis demonstrated that the polymers are thermally stable with the sequence shown in Scheme 2. This result is in agreement with TGA data as will be discussed below.

3.3.3. Physical properties

As the degree of crystallinity of a polymer affects its properties, accurately determining the crystallinity is important. There are various analytical methods used to determine the crystallinity of a polymer, namely, XRD, density, DSC, IR, and NMR [19]. XRD is used in this study. The crystallinity is measured by dividing the sum of the crystalline reflection intensities to the overall intensity. Fig. 4 shows the X-ray diffractogram of synthesized polymers. Gaussian curves are used to describe the amorphous phase and all crystal reflections of a diffractogram [20]. These curves are separated by computer-aided curve resolving technique. Percentage of crystallinity (X_c) is calculated as the ratio of crystalline area (A_c) to total area (A_c+A_a), where A_a is the amorphous area. The data are tabulated in Table 2. In Fig. 4, two distinct peaks with *d*-spacing of 0.414 and 0.373 nm are observed for all four polymers, as calculated from the Bragg equation. This demonstrated that all molecular chains are similar in conformation. One can see the intensity of diffraction peaks increases with the increase in the length of the flexible spacers. This indicates that the crystallinity of polymer increases with the length of flexible segments. This can be explained by the *trans* molecular conformation of polymer when the number of methylene units is even, molecules can be fitted easily into the crystal lattice and the rate of crystallization is faster as it cools down from the liquid crystal states [21].

Table 2
Crystallinity, viscosity, hygroscopicity, and LC phase of polymers

Polymer	Crystallinity X_c (%)	η_{inh}[a] (dL/g)	Hygroscopicity (%)	LC phase[b]
P1	19.52	0.42	0.361	Nematic
P2	27.15	0.35	0.416	Nematic
P3	18.33	0.38	0.247	Nematic
P4	25.77	0.54	0.377	Nematic
Vectra	28[c]	–[d]	0.1	Nematic

[a] 0.5 g/dL dissolves in NMP at 30 °C.
[b] Measured by POM.
[c] Hudson SD, Lovinger AJ. Polymer 1993;34:1124.
[d] Insoluble.

The inherent viscosities of the polymers ranged from 0.35 to 0.54 dL/g. They have good resistance to most solvents; P1 and P3 are only soluble in THF, NMP, and chloroform upon heating at 80 °C, while P2 and P4 must be heated up to 200 °C to be soluble (Table 3). Once cooled down to room temperature, all LCPs precipitate again. The difference in solubility can be attributed to the crystallinity associated with various LCPs. BDO containing polymers have higher crystallinity, which limits their solubilities. For Vectra, the high crystallinity makes it insoluble in solvents.

Low hygroscopicity is also critical for a polymer to be used in microelectronics. The measurements of hygroscopicity are tabulated in Table 2 with the values of 0.3–0.4%. This is resulted from the fact that the main chain

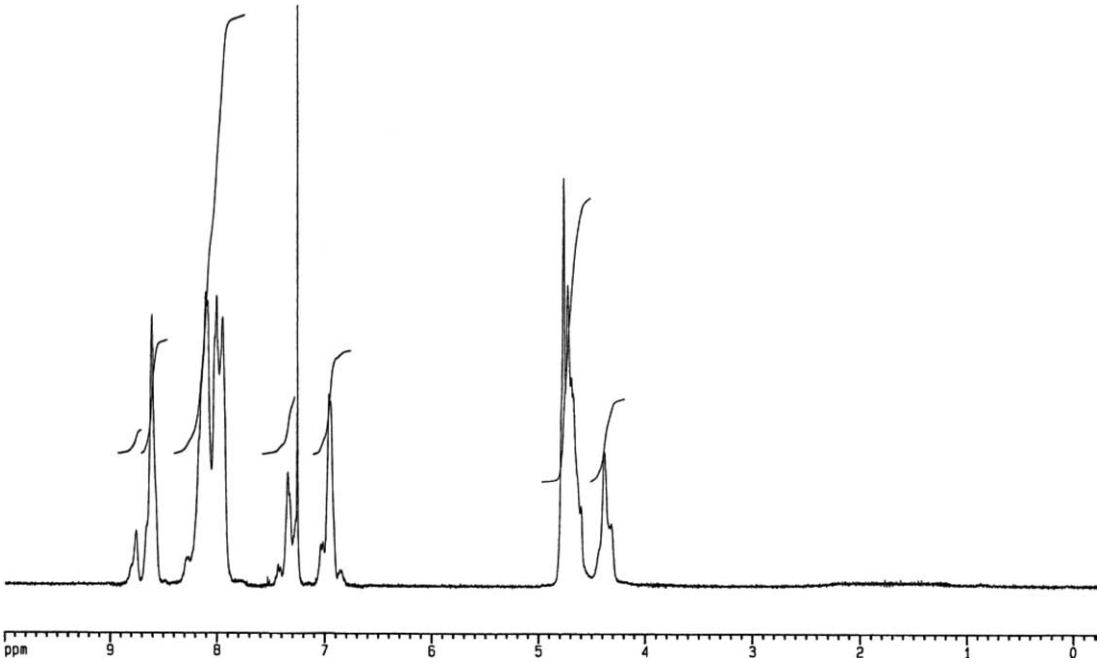

Fig. 3. ^{1}H NMR spectrum of P3.

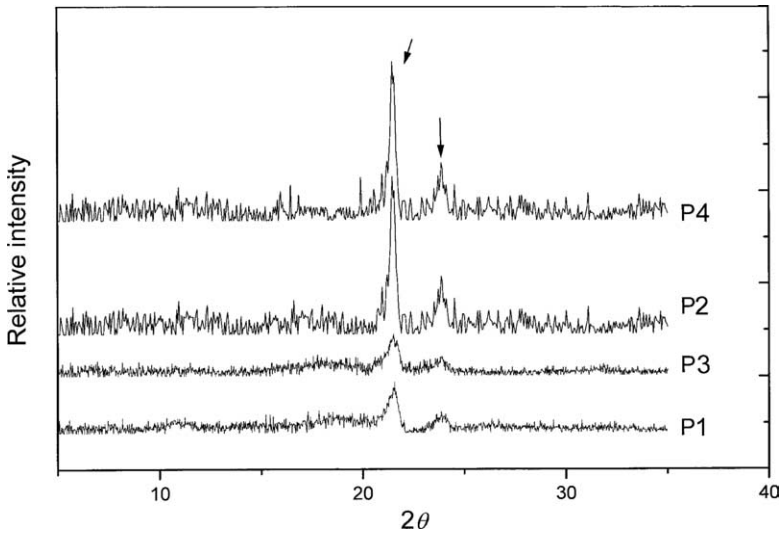

Fig. 4. X-ray diffractograms of liquid crystalline polymers.

molecules in the polymers are hydrophobic aromatic groups.

3.4. Thermal properties

Fig. 5 depicts TGA curves of the polymers. The two stages in the thermal decomposition curves is attributed to the fact that the main chain of the polymers is composed of aliphatic flexible segments and naphthalene containing rigid mesogenic chains. The aliphatic segments decomposed first, followed by the heat resistant aromatic chains. The thermal decomposition temperatures at 5 and 10% weight loss, $T_{d,5\%}$ and $T_{d,10\%}$, are all above 400 °C (under N_2 and air). This indicates that the synthesized LCPs have high thermal stability.

The glass transition temperature (T_g) of polymer is closely related to the flexibility of the chains because a high T_g is generally assumed to be connected with relatively high barriers of bond rotations [22]. The T_g measured by DSC is listed in Table 4. It showed that the T_g decreased with increased methylene units. These results indicated that the increase in the length of flexible spacers reduced the proportion of mesogens and decreased the rigidity of molecules. For the same flexible spacer, more mesogenic units containing naphthalene moiety have higher T_g due to the fact that naphthalene has better thermal stability [23]. These data are consistent with the results by dynamic

Table 4
Thermal properties of polymers

	P1	P2	P3	P4
$T_{d,5\%}$[a] (°C)	437 (435)	414 (414)	437 (437)	400 (408)
$T_{d,10\%}$[a] (°C)	451 (447)	428 (427)	447 (446)	413 (421)
$T_{d,max}$[a] (°C)	483 (475)	458 (453)	491 (488)	462 (461)
T_g[b] (°C)	103	74	105	88
T_g[c] (°C)	110	87	112	100
T_m (°C)	261	181	272	225
ΔH_m (J/g)	1.15	2.50	1.04	1.37
T_i[d] (°C)	>350	>350	>350	>350

[a] ( ): in air.
[b] Measured by DSC.
[c] Measured by DMA.
[d] Isotropic temperature.

Table 3
Solubilities of polymers

Solvent	P1	P2	P3	P4	Vectra
Chloroform	○	□	○	□	×
THF	○	□	○	□	×
DMAc	□	×	□	×	×
DMF	□	×	□	×	×
DMSO	×	×	×	×	×
NMP	○	□	○	□	×
p-Dioxane	×	×	×	×	×
Pyridine	○	×	○	×	×
m-Cresol	×	×	×	×	×
o-Xylene	×	×	×	×	×
Acetone	×	×	×	×	×
Ethyl alcohol	×	×	×	×	×

○, soluble in hot solvent; □, slightly soluble in hot solvent; ×, insoluble.

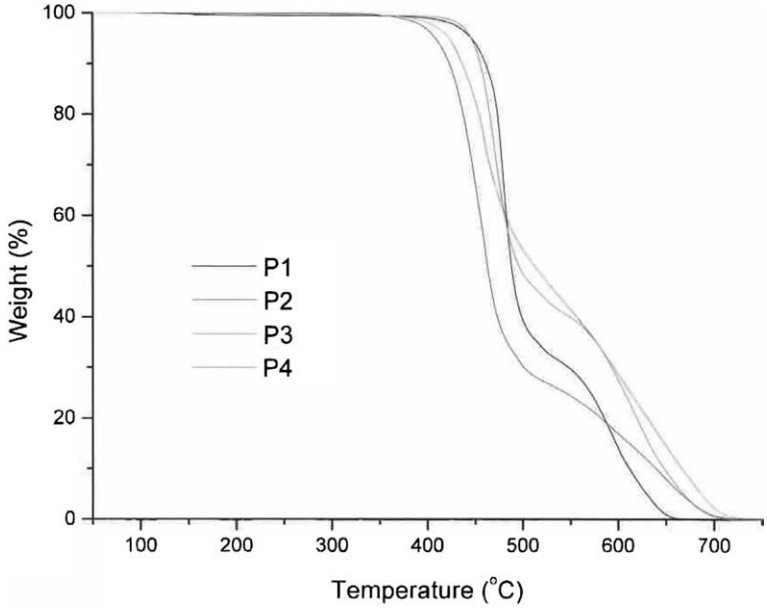

Fig. 5. TGA results of polymers under nitrogen.

mechanical analysis as also shown in Table 4. Fig. 6 illustrated a DMA diagram of P1. The T_g measured is 110 °C, which is the α relaxation peak of tan δ vs. temperature curve. The α relaxation corresponds to the materials changing from glassy state to a mobile nematic phase [24]. In all four LCPs synthesized, there is only one damping peak for each polymer. This elucidated good compatibility between the flexible spacers and rigid mesogens, and no obvious micro phase separation was observed.

The melting temperature (T_m) and heat of fusion (ΔH_m) of the LCPs were determined from the DSC heating thermograms. It was apparent that they all had lower T_m (for P2, only 181 °C) than Vectra (285 °C) and T_m tended to decrease with increasing crystallinity. This is significant for polymer processing in high performance engineering plastics applications, as a low T_m can facilitate extrusion or injection molding.

3.5. Liquid-crystalline behavior

Fibers were drawn as the polymers melted. The surface

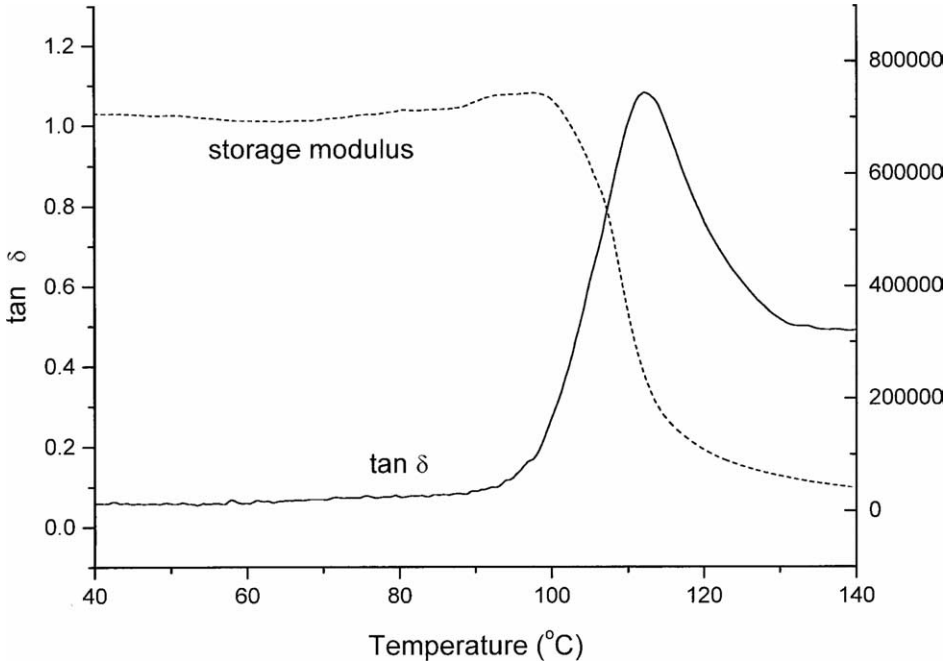

Fig. 6. DMA diagram of P1.

morphology was observed by SEM. It showed highly oriented LCP fibrils (Fig. 7(a)). The fiber surface was fractured cryogenically by liquid nitrogen, which revealed protruding fibrils uniformly distributed through the cross section with a diameter ~1 μm (Fig. 7(b)). The appearance of protruding fibrils on the fracture surface was consistent with the continuous fibril morphology of the LCP phase [25].

All the polymers formed turbid melts, and the melts exhibited strong stir opalescence at temperatures up to their transition into isotropic melt phases. Their isotropic temperatures, T_i, were very high and above the temperature limitation (>350 °C) in the heating apparatus. Thus, the T_i values could not be observed by POM. The optical textures of the polymers in the liquid-crystal states were observed with a polarizing microscope. Under POM, all of the polymers synthesized exhibited only nematic liquid crystalline mesophase at melt. The nematic structure is responsible for the low viscosity and the high degree of orientation. For P3, the marble texture was first observed on melting at 330 °C (Fig. 8(a)) and then changed to a thread texture at 290 °C (Fig. 8(b)). For polymer P2, which was synthesized from NDA, the schlieren texture at 285 °C changed to the droplet texture upon heating to 350 °C as shown in Fig. 9(a) and (b), respectively. Under cooling from isotropic melt, droplet texture grew into the schlieren texture of nematic mesophase as depicted in Fig. 9(c). Meanwhile, certain regions become dark indicated the isotropic liquid area. The mesophase temperature range ($\Delta T_{meso} = T_i - T_m$) was very broad (for P2, $\Delta T_{meso} > 160$ °C). This might be attributed to the presence of the crankshaft structure of the naphthalene in the LCPs that can decrease the degree of freedom of molecule movement, which results in a relatively broad range of mesophase. This is ideal for polymer processing in high performance engineering plastics applications.

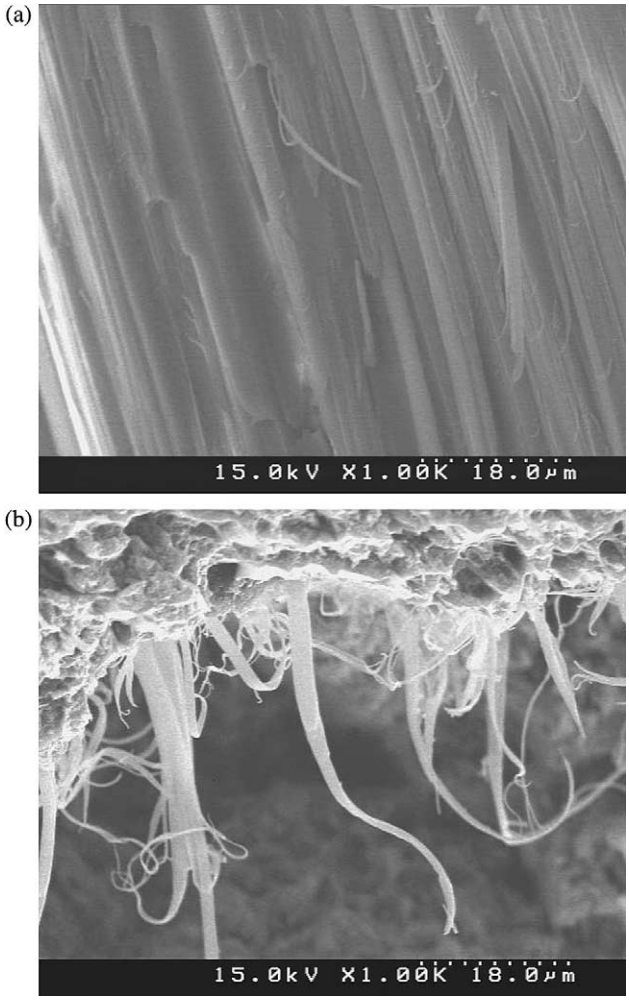

Fig. 7. (a) SEM micrograph of polymer (P2, 1000×). (b) Cryogenic fracture surface of P1 with 1000 magnification.

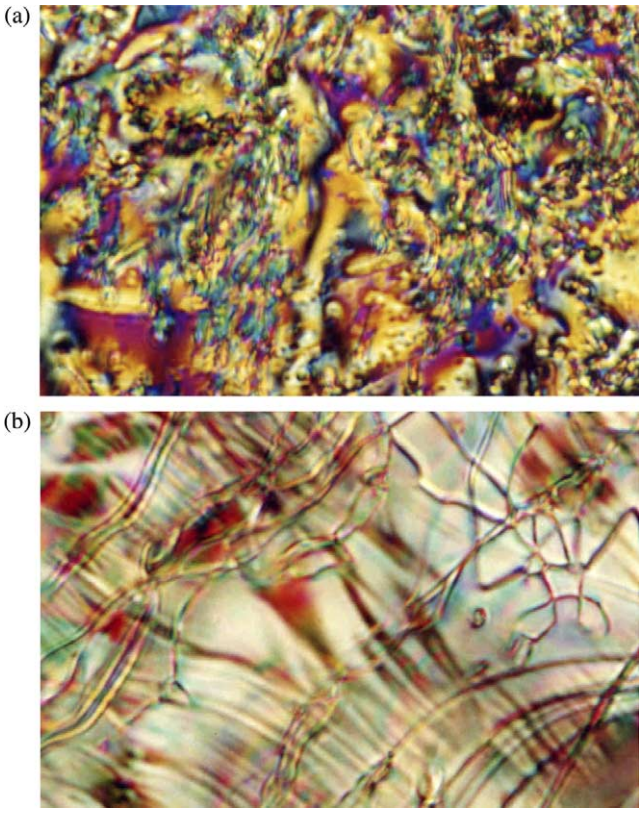

Fig. 8. Nematic mesophases of P3: (a) Marble texture at 330 °C (600×), and (b) thread texture at 290 °C (960×).

4. Conclusions

Four liquid crystalline polymers containing naphthalene mesogenic units and polymethylene spacers were successfully synthesized by melt polycondensation. NDA and TPA were used to substitute the expensive HNA and HBA in the raw material. The decomposition temperatures were all above 400 °C and the polymers had good solvent resistant. With the increase of polymethylene units in the spacer, the degree of crystallinity also increased, but the thermal properties decreased. The crankshaft structure of the

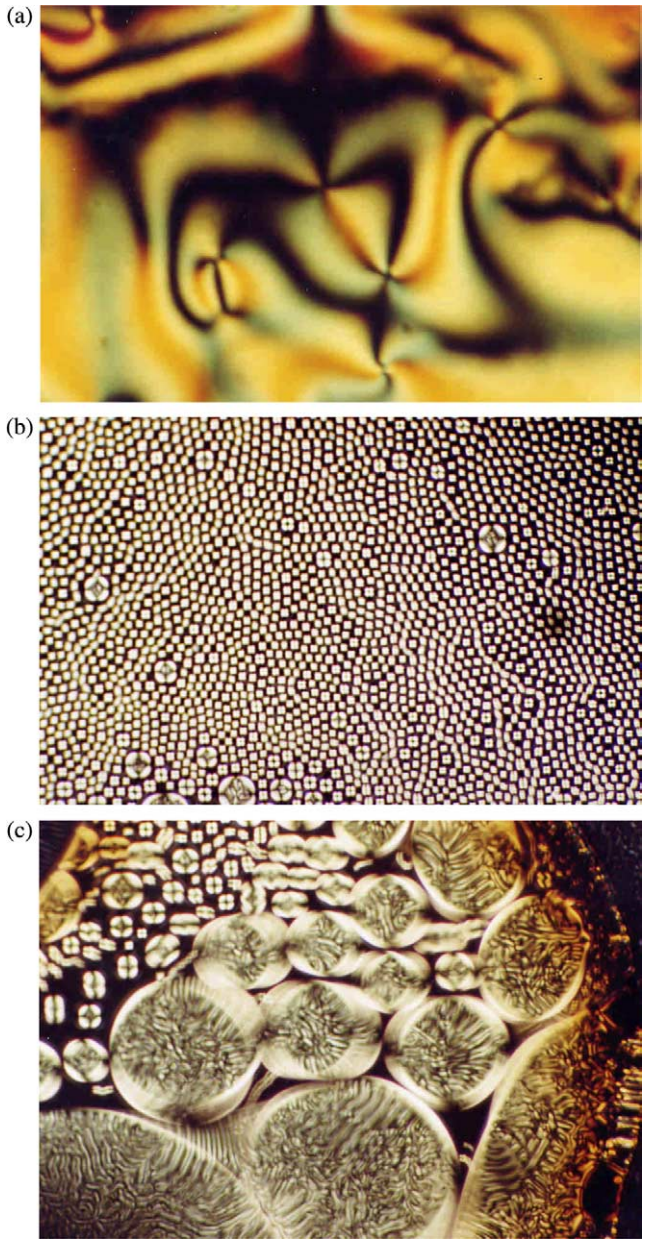

Fig. 9. Polarized optical micrographs of polymer P2. (a) Schlieren texture observed at 285 °C (600×), (b) changed to droplet texture upon heating to 350 °C (600×), and (c) became schlieren texture under cooling from isotropic melt (960×).

naphthalene in the LCP decreased the melting temperature of LCP to facilitate extrusion or injection molding. Under POM, they exhibited only nematic liquid crystal mesophase at melt and demonstrated a very broad mesomorphic temperature range. With these properties, low T_m, high crystallinity and broad ΔT_{meso}, and utilizing inexpensive raw materials, the novel LCPs exhibit improvements over Vectra in processability and cost. They have great commercial potential for application in microelectronics and high performance engineering plastics.

Acknowledgements

The authors thank the National Science Council of Taiwan for its financial support of this work (NSC94-2216-E-168-005) and the National Cheng Kung University for assistance in the characterization of polymer samples.

References

[1] Sun T, Lin YG, Winter HH, Porter RS. Polymer 1989;30(7):1257–61.
[2] Donald AM, Windle AH. Liquid crystalline polymers. Cambridge: Cambridge University Press; 1992.
[3] Collyer AA. Mater Sci Technol 1989;5:309.
[4] Kwolek SL. US Patent 3600350; 1971.
[5] Calundann GW. US Patents 4184996, 1980; 4256624, 1981.
[6] Yoon HN, Charbonneau LF, Calundann GW. Adv Mater 1992;4:206–14.
[7] Elsmer G, Rickel C, Zachmann HG. Adv Polym Sci 1985;67:1.
[8] Nakai A, Shiwaku T, Wang W, Hasegawa H, Hashimoto T. Polymer 1996;37(11):2259–72.
[9] Lenz RW. Polym J 1985;17:105–15.
[10] Tokita M, Osada K, Watanabe J. Polym J 1998;30:589–95.
[11] Zheng RQ, Chen EQ, Cheng SZD, Xie FC, Yan DH, He TB, et al. Macromolecules 1999;32:6981–8.
[12] Chang HS, Wu TY, Chen Y. J Appl Polym Sci 2002;83:1536–46.
[13] http://www.ticona.com/index/products/liquid_crystal.htm.
[14] Chung TA, Cheng SX. J Polym Sci, Part A: Polym Chem 2000;38:1257–69.
[15] Charbonneau LF. US Patent 4429105; 1984.
[16] Ravindranath K, Mashelkar RA. Chem Eng Sci 1986;41(9):2197–214.
[17] Cheng SX, Chung TS, Mullick S. Chem Eng Sci 1999;54(5):663–74.
[18] Catalgil-Giz H, Giz AT. Macromol Chem Phys 1994;195(3):855–64.
[19] Runt JP. In: Mark HF, Bikales NM, Overberger CG, Meges G, Kroschwitz J, editors. Encyclopedia of polymer science and engineering, vol. 4. New York: Wiley; 1986. p. 482.
[20] Wang ZG, Hsiao BS, Fu BX, Liu L, Yeh F, Sauer BB, et al. Polymer 2000;41(5):1791–7.
[21] Abe A. Macromolecules 1984;17:2280–7.
[22] Fernández-Blázquez JP, Bello A, Perez E. Macromolecules 2004;37:9018–26.
[23] Chen BK, Tsay SY, Shih IC. Polym Bull 2005;54:39–46.
[24] Tjong SC. Mater Sci Eng 2003;R41:1–60.
[25] Li JX, Silverstein MS, Hiltner A, Baer E. J Appl Polym Sci 1992;44:1531–42.